Ratchet transport of interacting particles

A. D. Chepelianskii,[1] M. V. Entin,[2] L. I. Magarill,[2] and D. L. Shepelyansky[3]

[1]*Laboratoire de Physique des Solides, UMR CNRS 8502, Bâtiment 510, Université Paris-Sud, 91405 Orsay, France*
[2]*Institute of Semiconductor Physics, Siberian Division of Russian Academy of Sciences, Novosibirsk, 630090, Russia*
[3]*Laboratoire de Physique Théorique–IRSAMC, UPS and CNRS, Université de Toulouse, 31062 Toulouse, France*

We study analytically and numerically the ratchet transport of interacting particles induced by a monochromatic driving in asymmetric two-dimensional structures. The ratchet flow is preserved in the limit of strong interactions and can become even stronger compared to the noninteracting case. The developed kinetic theory gives a good description of these two limiting regimes. The numerical data show emergence of turbulence in the ratchet flow under certain conditions.

I. INTRODUCTION

For systems without spatial inversion symmetry the appearance of directed flow of particles induced by a time-periodic parameter variation with a zero-mean force is now commonly known as the ratchet effect (see reviews [1–3]). This phenomenon is ubiquitous in nature so that such flows appear in a variety of systems including asymmetric crystals [4,5] and semiconductor surfaces [6] under light radiation, vortexes in Josephson junction arrays [7], macroporous silicon membranes [8], microfluidic channels [9], and others. A significant increase of interest to ratchets is related to the experimental progress in the investigation of molecular transport in biological systems such as proteins characterized by asymmetry and nonequilibrium [1–3]. At the same time the nanotechnology development allowed us to fabricate artificial asymmetric nanostuctures with the two-dimensional electron gas (2DEG) where it has been shown that infrared or microwave radiation creates a ratchet transport [10–13]. The theoretical studies predicted that the directionality of ratchet flow in such systems can be controlled by the polarization of radiation [14–18] that has been confirmed by recent experiments with a semidisk Galton board for 2DEG in AlGaAs/GaAs heterojunctions [19].

Until the present, the theoretical studies of ratchet transport have been performed mainly for noninteracting particles [1–5,14,18]. However, in many systems the interactions between particles are of primary importance, such as for example, for microfluidic channels [9], 2DEG nanostructures with strong electron-electron (e-e) interactions at a large r_s parameter [20], granulated materials [21], and one-dimensional Luttinger liquids [22]. On a first glance it seems that a strong scattering between particles should suppress the ratchet transport. On the other hand, the local conservation of momentum of particles indicates that even in the presence of strong interactions the ratchet flow still should exist. The investigation of the properties of ratchet transport for interacting particles in two dimensions is the main aim of this paper. The theory developed is based on the kinetic approach used in [18] extended to the case of strong interactions. The theory is compared with the extensive numerical simulations of ratchet transport of interacting particles in asymmetric structures. The model description is given in Sec. II; the

analytical theory based on the kinetic equation is developed in Sec. III; the numerical results are presented in Sec. IV and the discussion is given in Sec. V.

II. MODEL DESCRIPTION

The interactions between particles are treated in the frame of the mesoscopic multiparticle collision model (MMPCM) proposed by Kapral (see, e.g., [23]). This method exactly preserves the total momentum and energy of particles colliding inside each of N_{cel} collision cells on which the whole coordinate space with N particles is divided. In this method the collisions inside cells are modeled by rotation of all particle velocities in the moving center-of-mass frame of a given cell on a random angle after a time τ_K. To equilibrate the whole system of interacting particles in the presence of external monochromatic driving force $\mathbf{F} \cos \omega t$ we use the Nosè-Hoover thermostat [24] which drives the system to the Boltzmann equilibrium with a temperature $T = m v_T^2/2$ on a relaxation time τ_H. Such a combination of two methods for systems with interactions and ac driving has been already used in [25]. As in [18] the asymmetry appears due to asymmetric scatterers having the form of vertical cuts with diffusive (right-hand) and elastic (left-hand) sides (cuts model) or of elastic semidisks of radius r_d (semidisks model) placed in a periodic square lattice of size $R \times R$. The system orientation geometry and two types of scatterers are shown in Fig. 1 (see also [18] and Fig. 5 below). In the cuts model it is assumed that the scattering on cuts takes place instantaneously at random moments of time which have a Poisson distribution with
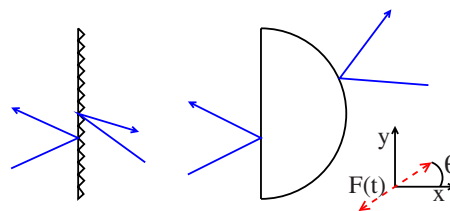

FIG. 1. (Color online) Geometry of asymmetric scatterers oriented in the (x,y) plane: Cuts with elastic (left-hand) and diffusive (right-hand) sides; elastic semidisks; linear-polarized force $\mathbf{F}$ has angle θ with respect to the x axis.
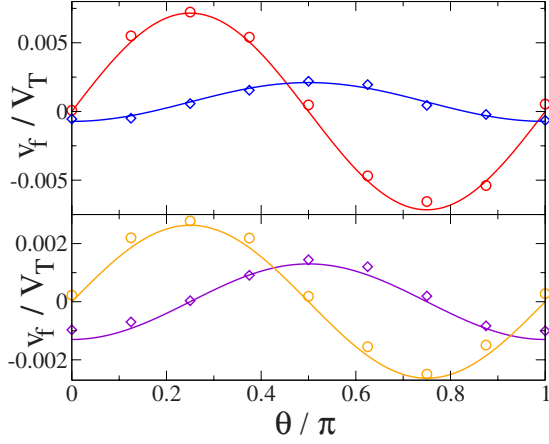
FIG. 2. (Color online) Polarization dependence of the average ratchet flow $\mathbf{v_f}$ in the flashing cuts model with (top panel) and without (bottom panel) interactions; diamonds and circles show numerical data for $v_{f,x}$ and $v_{f,y}$ components, curves give the fits of data (see text). The system parameters are $N=10^4$, $N_{cel}=100 \times 100$ inside the periodic space domain $R \times R$ with $v_T \tau_H/R=2.4$, $\tau_c/\tau_H=0.45$, $\tau_K/\tau_H=0.02$, $\omega\tau_H=3$, $Fv_T\tau_c/T=0.64$ for the top panel and the same parameters for the bottom panel but $\tau_K/\tau_H=\infty$ and impurity scattering is added with $\tau_{im}/\tau_H=0.5$; total integration time is $t/\tau_H \approx 10^3$.

time scale τ_c. This corresponds to the case of the flashing cuts model (instantaneous appearance of cut at some moment of time) which is slightly different from the case of static cuts randomly distributed in the plane (both cases were discussed in [18]). As in [18], in absence of interactions an effective impurity scattering is added with the scattering time τ_{im}. The monochromatic force is polarized as it is shown in Fig. 1 with $\mathbf{F}=F(\cos\theta, \sin\theta)$. Here, we present numerical results only for the semidisks model and the flashing cuts model, which is rather convenient for numerical simulations, but in the analytical treatment we also consider the static cuts model.

The results of numerical simulations for the polarization dependence of the ratchet flow in the flashing cuts model are shown in Fig. 2. In the absence of interactions the results are well described by the theory [18] with the fit dependence $\mathbf{v_f}/v_T=b[-\cos(2\theta), 2\sin(2\theta)]/2$, where $b=0.0064 \times (Fv_T\tau_c/T)^2 \approx 0.8b_{th}$ and b_{th} is the theory value [see Eqs. (9) and (41) in [18]]. For interacting particles the fit gives the dependence $\mathbf{v_f}/v_T=b_{int}[-a_1\cos^2\theta+a_2\sin^2\theta, \sin(2\theta)]$ with $b_{int}/b=2.7$ and $a_1=0.10$, $a_2=0.29$. In the presence of interactions the ratchet flow appears even after polarization averaging. The results for the semidisks model are shown in Fig. 3. Without interactions the data are satisfactory described by the theoretical dependence $\mathbf{v_f}/v_T=b[-\cos(2\theta), \sin(2\theta)]$ with the fitting value $b=0.24(Fr_d/T)^2 \approx 0.4b_{th}$ and the theoretical value b_{th} of [18] [see Eq. (42) and discussion there]. In the presence of interactions, the polarization dependence of the flow is qualitatively changed: The component v_y is enhanced by a factor of 8 and v_x remains negative for all θ showing a signature of the fourth θ harmonic (Fig. 3, top panel, curves are shown as a guide for the eye).
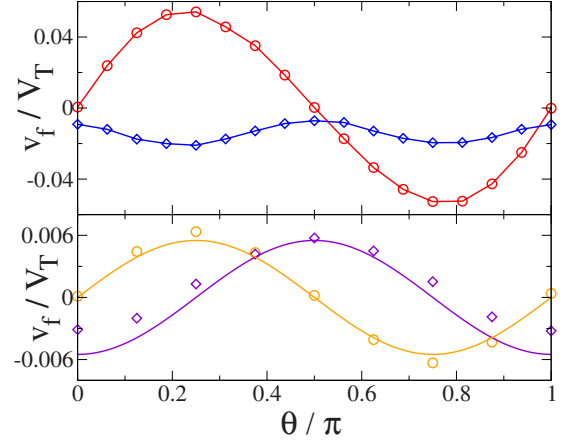

FIG. 3. (Color online) Same as in Fig. 2 for the semidisk model with $R/r_d=4$, $Fr_d/T=0.15$, $\omega\tau_H=1$, effective $\tau_c/\tau_H \approx R^2/(2r_d v_T\tau_H)=0.85$, other parameters are as in Fig. 2.

III. ANALYTICAL THEORY

The numerical simulations are based on the dynamical description of motions of many interacting particles. To obtain an analytical description of the ratchet transport we use the kinetic equation approach valid for systems with developed chaos and rapid decay of correlations. The validity of the kinetic equation requires rare collisions with asymmetric scatterers (antidots) and randomness of scattering events. Under such conditions the kinetic equation can be applied for comparative study with the numerical data even if the numerical simulations are done for a deterministic system with a periodic lattice of semidisks of relatively large size.

The symmetry of the system determines the ratchet flow which mean velocity $\mathbf{v}_f$ is quadratic in the amplitude of the ac force $\mathbf{F}(t)=\mathrm{Re}(\mathbf{F}e^{-i\omega t})$. Therefore, the flow velocity can be described by the phenomenological expressions

$$v_{f,x} = \alpha_{xxx}|F_x|^2 + \alpha_{xyy}|F_y|^2, \quad v_{f,y} = 2\,\mathrm{Re}(\alpha_{yxy}F_x F_y^*).$$

The tensor components α_{xxx}, α_{xyy}, and $\mathrm{Re}(\alpha_{yxy})$ determine the response produced by a linear-polarized monochromatic force (Im $\mathbf{F}=0$). In the absence of interactions (see [18]), for the linear polarization along the x or y axes, the mean flow is directed along the x axis; the current in the y direction appears for a tilted linear-polarized force.

We also note that for the elliptically polarized force with Im $\mathbf{F} \neq 0$ there exists also a circular ratchet effect determined by the product of $\mathrm{Im}(\alpha_{yyx})$ and $\mathrm{Im}(F_x F_y^*)$ but we will not consider this effect here.

A. Kinetic equation

The kinetic equation in the momentum space $\mathbf{p}$ reads as

$$\frac{\partial f}{\partial t} + \mathbf{F}(t)\frac{\partial f}{\partial \mathbf{p}} = \hat{I}(f), \qquad (1)$$

where in the case of microwave field, $\mathbf{E}(t)$ is the electric field interacting with electron gas $\mathbf{F}(t)=e\mathbf{E}(t)$, e is the electron charge. The collision operator $\hat{I}=\hat{I}_{el}+\hat{I}_{ee}$ contains the operator

of elastic collisions [including impurities and scatterers (or antidots)] $\hat{I}_{el}$ and interparticle (electron-electron or *e-e*) collisions $\hat{I}_{ee}$.

The integral of elastic collisions with scatterers and static impurities reads as

$$\hat{I}_{el}(f_{\mathbf{p}}) = \sum_{\mathbf{p}'} Q_{\mathbf{p}\mathbf{p}'} f_{\mathbf{p}'} = \sum_{\mathbf{p}'} [W(\mathbf{p}',\mathbf{p}) f_{\mathbf{p}'} - W(\mathbf{p},\mathbf{p}') f_{\mathbf{p}}], \quad (2)$$

where $Q_{\mathbf{p}\mathbf{p}'}$ is the kernel of the operator $\hat{I}_{el}$ and $W(\mathbf{p}',\mathbf{p})$ is the probability of the transition from $\mathbf{p}'$ to $\mathbf{p}$.

The interparticle collisions operator (*e-e*) is

$$\hat{I}_{ee}(f) = \frac{2\pi}{S^2} \sum_{\mathbf{p}_1, \mathbf{p}', \mathbf{p}_1'} \delta_{\mathbf{p}+\mathbf{p}_1, \mathbf{p}'+\mathbf{p}_1'} \delta(\epsilon_{\mathbf{p}} + \epsilon_{\mathbf{p}_1} - \epsilon_{\mathbf{p}'} - \epsilon_{\mathbf{p}_1'}) u_{\mathbf{p}-\mathbf{p}'}^2$$

$$\times [f_{\mathbf{p}'} f_{\mathbf{p}_1'} (1-f_{\mathbf{p}})(1-f_{\mathbf{p}_1}) - f_{\mathbf{p}} f_{\mathbf{p}_1} (1-f_{\mathbf{p}'})(1-f_{\mathbf{p}_1'})]. \quad (3)$$

Here, S is the sample area and $u_{\mathbf{k}}$ is the Fourier transform of *e-e*-interactions.

Interparticle collisions satisfy the conservation of the total momentum of gas. Due to the Galileo invariance the action of the collision integral on the equilibrium distribution function with shifted argument $\hat{I}_{ee} f_{\mathbf{p}+\mathbf{a}}^{(0)}$ vanishes for any $\mathbf{a}$. Expanding by $\mathbf{a}$ we have

$$\hat{I}_{ee}(f_{\mathbf{p}}^{(0)}) = 0, \quad \hat{I}_{ee}'(\mathbf{a}\partial_{\mathbf{p}} f^{(0)}) = 0,$$

$$\hat{I}_{ee}''(\mathbf{a}\partial_{\mathbf{p}} f^{(0)} * \mathbf{a}\partial_{\mathbf{p}'} f^{(0)}) + \hat{I}_{ee}'(a_i a_j \partial_{p_i, p_j}^2 f^{(0)}) = 0. \quad (4)$$

We use the following notations for the first and the second variations around equilibrium: $\delta\hat{I}_{ee}(f) = \hat{I}_{ee}'(\delta f)$ (linear operator), $\delta^2\hat{I}_{ee}(f) = \hat{I}_{ee}''(\delta f * \delta f)$ (bilinear operator, asterisk denotes integration with two functions of different arguments).

The ratchet flow is generated by the anisotropy of collisions. This anisotropy is constructed artificially due to the asymmetric form of oriented scatterers. As theoretical models we considered cases of fixed oriented anisotropic scatterers, namely cuts and semidisks. The model of static cuts is analytically solvable [18] but has a disadvantage since it leads to a divergence due to electrons moving along the mirrors. Even if this divergence can be regularized by an isotropic impurity scattering such a property is not very convenient. Owing to that, it is useful to use a modified model of flashing cuts which does not have such divergence. In this model at any moment a particle can meet a scatterer with a constant probability independent of its velocity and direction of motion; after collision the particle equiprobably scatters into any angle of the right-hand semicircle if it collides from the right-hand semicircle and is mirror-reflected if it collides from the left-hand semicircle (see Fig. 1). Such a model of flashing cuts gives a significant simplification for analytical and numerical studies.

The corresponding transition probability in these models is given by (see also [18])

$$W(\mathbf{p}',\mathbf{p}) = \frac{4\pi^2}{mS} w(\varphi',\varphi) \delta(\varepsilon_{\mathbf{p}} - \varepsilon_{\mathbf{p}'}); \quad (5)$$

with

$$w(\varphi',\varphi) = \frac{1}{\tau_c} \left(\cos\varphi' \, \theta(\cos\varphi') \delta(\varphi' + \varphi - \pi) \right.$$
$$\left. - \frac{1}{2} \cos\varphi' \cos\varphi \, \theta(\cos\varphi) \theta(-\cos\varphi') \right)$$
$$\text{(static cuts)}, \quad (6)$$

$$w(\varphi',\varphi) = \frac{1}{\tau_c} \left[\cos\varphi' \, \theta(\cos\varphi') \delta(\varphi' + \varphi - \pi) \right.$$
$$+ \frac{1}{4} \left| \sin\left(\frac{\varphi - \varphi'}{2} \right) \right| [\theta(\varphi - \varphi') \theta(-\varphi - \varphi')$$
$$\left. + \theta(\varphi' - \varphi) \theta(\varphi + \varphi')] \right] \quad \text{(semidisks)}, \quad (7)$$

$$w(\varphi',\varphi) = \frac{1}{\tau_c} \left[\theta(\cos\varphi') \delta(\varphi' + \varphi - \pi) \right.$$
$$\left. + \frac{1}{\pi} \theta(\cos\varphi) \theta(-\cos\varphi') \right] \quad \text{(flashing cuts)}.$$
$$(8)$$

Here ϕ is the polar angle of electron momentum $(-\pi < \phi < \pi)$, $\tau_c(\varepsilon)$ is the characteristic scattering time on asymmetric scatterers, $\theta(x)$ is the Heaviside function.

B. Linear response

We consider the limit of a high rate of interparticle scattering exceeding the rate of elastic collisions. At the same time the interactions preserve the total momentum and in isotropic media do not affect the momentum relaxation. This is not the case for an anisotropic medium where the interactions indirectly lead to the momentum relaxation due to the conversion of the first angular harmonic of the distribution function $f_{\mathbf{p}}$ to higher harmonics produced by the anisotropic scattering. In particular, it is generally excepted that in an isotropic medium with closed Fermi surface the *e-e* scattering does not affect the conductivity. Nevertheless, in the considered case of anisotropic medium *e-e* collisions indirectly affect the momentum relaxation rate. This action is realized due to the conversion of the first angular harmonics of the distribution function to higher harmonics produced by the anisotropic scattering. As a result, the conductivity becomes temperature dependent in the temperature range when the *e-e* relaxation time is comparable with the elastic relaxation time.

At first we consider the linear response to the electric field using the expansion $f = f^{(0)} + f^{(1)} + f^{(2)} + \cdots$ in small driving force F. The linearized kinetic equation can be written in the form $[f^{(1)}(t) = \text{Re}(f_\omega^{(1)} e^{i\omega t})]$

$$-i\omega f_\omega^{(1)} + \mathbf{F}_\omega \partial_{\mathbf{p}} f^{(0)} = \hat{I}^{(1)}(f_\omega^{(1)}), \qquad (9)$$

where the collision operator contains the elastic collisions with anisotropic scatterers determined by $\hat{I}_{el}$ and interparticle or *e-e* collisions determined by $\hat{I}'_{ee}$;

$$\hat{I}^{(1)} = \hat{I}_{el} + \hat{I}'_{ee}. \qquad (10)$$

The formal solution of Eq. (9) in the first order of alternating force is

$$f_\omega^{(1)} = (i\omega + \hat{I}^{(1)})^{-1}(\mathbf{F}_\omega \partial_{\mathbf{p}}) f^{(0)}. \qquad (11)$$

In the case of weak *e-e* interaction $\hat{I}_{ee}$ can be canceled. In the opposite limit of strong *e-e* scattering the formal parameter describing $\hat{I}_{ee}$ is large. Having in mind Eq. (4) we see that the inverse operator $(\omega + \hat{I}^{(1)})^{-1}$ can be found by a projection on the subspace of the Hilbert space of the basis functions $\psi_i = \frac{\partial f^{(0)}}{\partial p_i} / \|\frac{\partial f^{(0)}}{\partial p_i}\|$ corresponding to zero eigenvalue of the operator $\hat{I}'_{ee}$. Thus, the operator $\hat{I}_{el}$ is replaced by its projection, while $\hat{I}'_{ee}$ can be canceled. The resulting tensor of conductivity of *e*-charged particles with density n_e reads as

$$\sigma_{ij}(\omega) = \frac{e^2 n_e}{m} \frac{\tau_i}{1 - i\omega\tau_i} \delta_{ij}, \qquad (12)$$

where τ_i are relaxation times of the first harmonics of the distribution function related with the projected operator of elastic collisions,

$$\frac{1}{\tau_i} = -\sum_{\mathbf{p},\mathbf{p}'} \psi_i(\mathbf{p}) Q_{\mathbf{p}\mathbf{p}'} \psi_i(\mathbf{p}'). \qquad (13)$$

Here in the τ_i index, i is the axis index (x or y). For the considered systems from the relations (6)–(8) we have $\tau_i = \bar{\tau}_c / a_i$ and

$$a_x = \frac{\pi}{8} + \frac{4}{\pi}, \quad a_y = \frac{2}{3\pi} \quad \text{(for static cuts)},$$

$$a_x = \frac{2}{3} + \frac{8}{3\pi}, \quad a_y = \frac{2}{3} \quad \text{(for semidisks)},$$

$$a_x = \frac{3}{2} + \frac{4}{\pi^2}, \quad a_y = \frac{1}{2} \quad \text{(for flashing cuts)}. \qquad (14)$$

The quantity $\bar{\bar{\tau}}_c$ is determined by gas statistics

$$\frac{1}{\bar{\bar{\tau}}_c} = \frac{\int_0^\infty d\varepsilon (f^{(0)\prime})^2 [\varepsilon/\tau_c(\varepsilon)]}{\int_0^\infty d\varepsilon \varepsilon (f^{(0)\prime})^2},$$

where the prime denotes the derivative over the energy ϵ.

In the case of static cuts or semidisks $1/\tau_c(\varepsilon) \propto \varepsilon^s$ with $s = 1/2$. So, one can write $\bar{\bar{\tau}}_c = \tau_c(\varepsilon_F)$ (strongly degenerate Fermi case) and $\bar{\bar{\tau}}_c = 4\sqrt{2/\pi}\tau_c(T)/3$ (Boltzmann case); $s = 1/2$ for fixed obstacles and $s = 0$ for flashing cuts [in this case $\tau_c(\varepsilon) = \text{const}$].

The physical origin of Eqs. (12) and (13) is a very quick relaxation of higher angular momenta harmonics as compared to the first harmonic relaxation. As a result, the conductivity has different values at low temperature, when $\tau_{ee} \gg \tau_{el}$ and at high temperature when $\tau_{ee} \ll \tau_{el}$. In both limits the conductivity does not depend on *e-e* interaction, but has different values. In the case of the Fermi distribution the conductivity changes from low-temperature value where $\tau_{ee} \gg \tau_{el}$ to high-temperature value where $\tau_{ee} \ll \tau_{el}$. We should emphasize that the transition between these two values is ruled by the ratio τ_{ee}/τ_{el} rather than by the ratio of temperature T to the Fermi energy E_F. The transition temperature T_0 can be estimated by equating *e-e* relaxation time to the relaxation time given by elastic scattering. In clean samples with high mobility the transition corresponds to a rather low temperature $T_0 \sim E_F / \alpha \sqrt{\lambda_F / l_p}$, where $\alpha = (e^*)^2 / \hbar v_F$ is the dimensionless *e-e* interaction constant, λ_F and v_F are the Fermi wavelength and velocity l_p is the elastic mean free path. For $E_F = 0.01$ eV, $\lambda_F \approx 10$ nm, $\alpha = 0.5$, $l_p \sim 10^{-4}$ cm, $T_0 \sim 10$ K.

From Eq. (12) one can write the expression for the ratio of static conductivities σ_{yy}/σ_{xx},

$$\sigma_{yy}/\sigma_{xx} = \tau_y/\tau_x = a_x/a_y. \qquad (15)$$

In the case of flashing cuts this ratio is equal to $3 + 8/\pi^2 \approx 3.81$ [see Eq. (14)]. For such scatterers the problem of linear conductivity is solved exactly also in the limit of absence of *e-e* interaction (see, e.g., [18]). Using Eq. (8), we find $\sigma_{ii} = n_e e^2 \tau_c b_i / m$, $b_x = 1/2$, $b_y = 3/2$. Thus, in this case $\sigma_{yy}/\sigma_{xx} = 3$. Hence, for example, for this flashing cuts model the ratio $\sigma_{yy}/\sigma_{xx} = 3$ is changed significantly when the temperature is changed from $T < T_0$ to $T > T_0$.

C. Quadratic response

The stationary ratchet flow appears in the second order of ac force F. In this case we can operate in a similar way as before. The nonlinearity occurs due to the field term in the kinetic equation and nonlinear *e-e* collision operator

$$\partial_t f^{(2)} - (\hat{I}_{el} + \hat{I}'_{ee})(f^{(2)}) = -[\mathbf{F}(t)\partial_{\mathbf{p}}]f^{(1)} + \hat{I}''_{ee}(f^{(1)} * f^{(1)}). \qquad (16)$$

The projection of anisotropic elastic collision operator onto the vector functions kills the third rank tensor needed for photogalvanic current. So inclusion of anisotropy should be done a bit more accurately. In short, the stationary ratchet current is generated in the following way. The oscillating distribution function with vector anisotropy is converted by nonlinear *e-e* interactions to the static second angular harmonics which in turn is partially suppressed by linear *e-e* interactions and then is transformed to the static vector anisotropy by anisotropic elastic collisions. The main contribution to the stationary flow reads as

$$j_i = \frac{1}{S} \text{Re} \sum_{\mathbf{p}} v_i \hat{I}^{-1} \hat{I}^{(-)} \hat{I}^{-1} \hat{I}_{ee}^{(2)}(f_{-\omega}^{(1)} * f_\omega^{(1)}). \qquad (17)$$

Equation (17) has a simplified form in accordance with the smallness of the elastic antisymmetric operator $\hat{I}^{(-)}$ as com-

pared with the inelastic scattering ($\hat{I}^{(-)}$ obligatory contains higher angular harmonics). The subsequent simplifications include the following: The substitution of $\hat{I}'_{ee}$ instead of $\hat{I}''_{ee}$, according Eq. (4); use of the fact that inverse operators $\hat{I}^{-1}$ do not contain antisymmetric operators; the cancellation of $\hat{I}^{-1}\hat{I}^{(1)}_{ee}$ acting on the second angular harmonics; the replacement of the left-hand operator $\hat{I}^{-1}$ (taking into account summation with v_i) by the inverse projected operator. As a result, we arrive at

$$v_{f,i} = -\frac{1}{2}C\sum_{j,k} a_{jki}\tau_i \, \mathrm{Re}(\tau_{\omega j}\tau^*_{\omega k}F_{\omega j}F^*_{\omega k}). \qquad (18)$$

Here $\varepsilon = mv^2/2$ is the particle energy, $a_{ijk} = \langle v_i v_j \hat{I}^{(-)} v_k \rangle \tau_c / v^3$ is a numerical tensor, characterizing the asymmetry of scatterers ($\langle \cdots \rangle$ stands for average over angles in the momentum space), prime again means the derivative over particle energy, $1/\tau_{\omega i} = -i\omega + 1/\tau_i$. For the specific cases of our models we obtain

$$a_{xxx} = \frac{1}{48}, \quad a_{xyy} = -\frac{1}{16} \quad \text{(for static cuts)},$$

$$a_{xxx} = -a_{xyy} = \frac{1}{12} \quad \text{(for semidisks)},$$

$$a_{xxx} = \frac{1}{6\pi}, \quad a_{xyy} = -\frac{1}{3\pi} \quad \text{(for flashing cuts)}. \qquad (19)$$

For C we have

$$C = \frac{\displaystyle\int_0^\infty d\varepsilon (f^{(0)'})^2 (v^3/\tau_c)'}{\displaystyle\int_0^\infty d\varepsilon\, \varepsilon (f^{(0)'})^2}.$$

In the case of static cuts or semidisks $C = (3/2 + s)v_F^3 / [\tau_c(\varepsilon_F)\varepsilon_F^2]$ (strongly degenerate Fermi case) and $C = 2d_s(3/2+s)/[2^{1/2+s}m\tau_c(T)\sqrt{mT}]$ (Boltzmann case); $s = 1/2$, $d_s = 1$ for fixed obstacles and $s = 0$, $d_0 = \sqrt{\pi}/2$ for flashing cuts [in this case $\tau_c(\varepsilon) = \mathrm{const}$].

To compare with results of numerical calculations it is convenient to write expressions for ratchet velocity components. For the linear polarization of monochromatic force we obtain

$$v_{fx}/v_T = -B(Fv_T\bar{\tau}_c/T)^2 a_{xxx}$$
$$\times \{\cos^2\theta/[a_x^3(1+\omega^2\tau_x^2)] - \sin^2\theta/[a_x a_y^2(1+\omega^2\tau_y^2)]\},$$

$$v_{fy}/v_T = -B(Fv_T\bar{\tau}_c/T)^2 a_{xyy}$$
$$\times \sin(2\theta)(1+\omega^2\tau_x\tau_y)/[a_x a_y^2(1+\omega^2\tau_x^2)(1+\omega^2\tau_y^2)], \qquad (20)$$

where $B = CT^2\bar{\tau}_c/2v_T^3$ and we remind the reader that $\tau_i = \bar{\tau}_c/a_i$. For the flashing cuts model we have $\tau_c = \bar{\tau}_c$, $a_{xxx} = 1/6\pi$, $a_{xyy} = -1/3\pi$, $a_x = 3/2 + 4/\pi^2$, $a_y = 1/2$, $C = 2\sqrt{\pi}/(2m\tau_c\sqrt{2mT})$, $\tau_c = \mathrm{const}$ and for the semidisks model
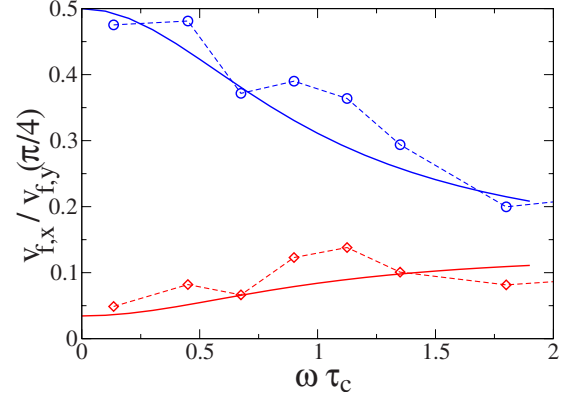

FIG. 4. (Color online) Comparison between theory (20) (full curves, no adjustable parameters) and numerical data for interacting particles in the flashing cuts model (symbols); circles are for $v_{f,x}$ and $\theta = \pi/2$ (here $v_{f,x} > 0$), diamonds are for $|v_{fx}|$ and $\theta = 0$ [here $v_{f,x} < 0$ and we use the absolute value of $v_{f,x}$ in the ratio $v_{f,x}/v_{f,y}(\pi/4)$]; $v_{f,y}$ is taken at $\theta = \pi/4$; other parameters are as in Fig. 2, top panel.

$a_{xxx} = -a_{xyy} = 1/12$, $a_x = 2/3 + 8/3\pi$, $a_y = 2/3$, $C = 2/(m\bar{\tau}_c\sqrt{mT})$, $\bar{\tau}_c \propto T^{-1/2}$. Here we give the results for the Boltzmann distribution $f^{(0)}$, but similar calculations work for other $f^{(0)}$, e.g., for the Fermi-Dirac distribution. We also give a simplified derivation of the ratchet flow in the Appendix. It is based on the local equilibrium distribution and give the same results as Eqs. (20).

The opposite limit in the absence of e-e interactions was analytically studied for the cases of static cuts [16] (exactly) and approximately, for weak anisotropy, for static cuts or semidisks [18]. It is important to emphasize that in both limits of weak and strong e-e interactions the current does not contain the strength of interactions. The transition between the regimes occurs when the interparticle scattering rate becomes comparable with the rate elastic scattering on antidots and impurities.

IV. NUMERICAL RESULTS

For the flashing cuts model the theory (20) gives a good description of numerical data (see Fig. 4). For the semidisks model the agreement between the theory and numerical simulations (Fig. 3, top) is less accurate, e.g., fourth θ harmonic for $v_{f,x}$ is absent in (20). To understand the origins of this difference we present the map of local flow velocities at various polarizations θ in Fig. 5. For $\theta = 0$ the results clearly show the appearance of turbulent flow with two vertexes behind the semidisk. When the interaction scattering time τ_K is increased by a factor 25 the interaction and turbulence practically disappear and the average local flow becomes laminar (see Fig. 5 top left-hand and bottom right-hand panels). At the same time even with strong interactions the flow has much more laminar structure for $\theta = \pi/4$ (Fig. 5, top right-hand panel) when the absolute value of the total ratchet velocity has its maximal value (see Fig. 3 top panel). Thus, the ratchet flow of interacting particles has certain similarities with a hydrodynamic flow of the Navier-Stocks equation
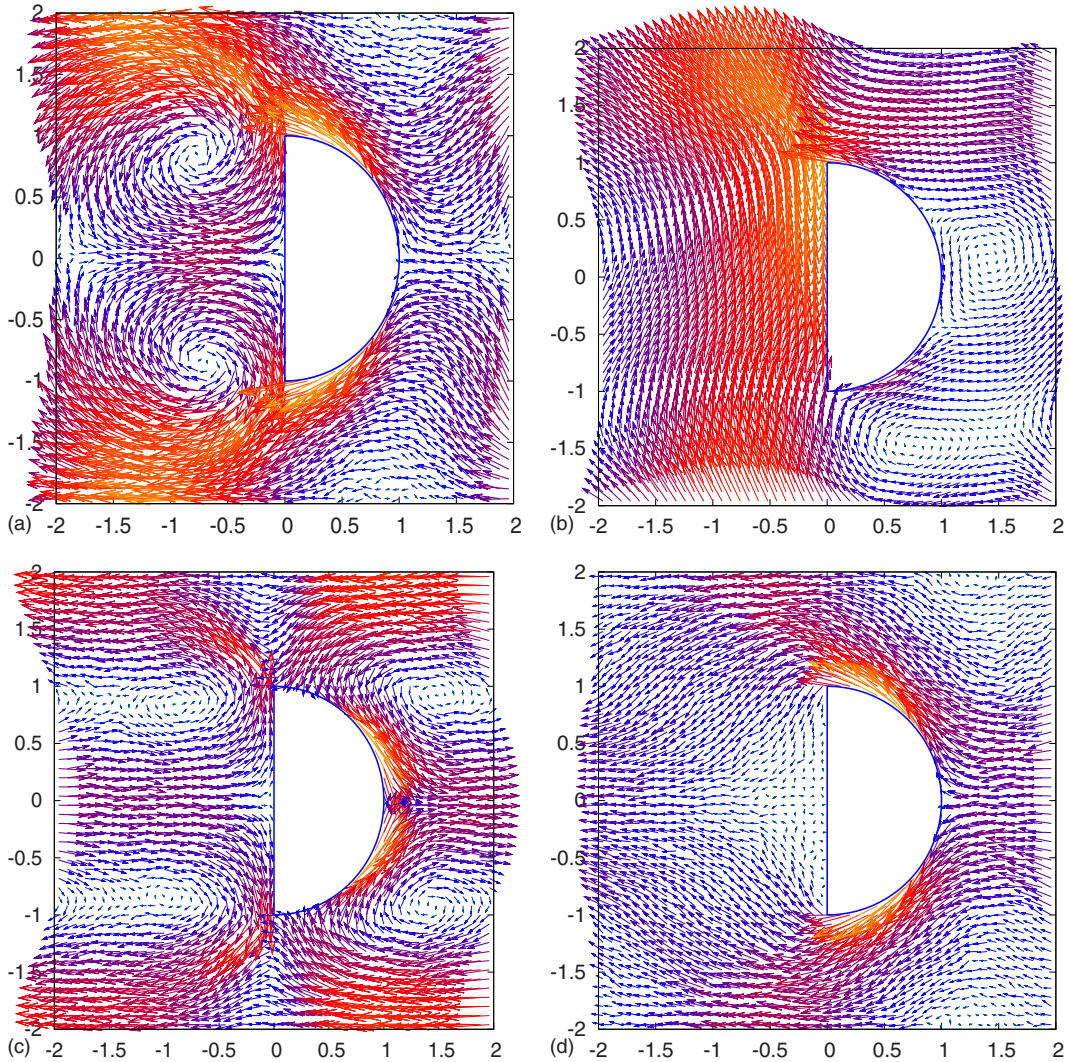
FIG. 5. (Color online) Map of local averaged velocities in $(x/R, y/R)$ plane of the semidisks model for parameters of Fig. 3 (top panel) at $\theta=0$ (top left-hand side); $\theta=\pi/4$ (top right-hand side); $\theta=\pi/2$ (bottom left-hand side); $\theta=0$ and 25 times increased interaction time compared to other panels ($\tau_K/\tau_H=0.5$, $\tau_K v_T/r_d=4.7$ point in Fig. 6). The velocities are shown by arrows which size is proportional to the velocity amplitude, which is also indicated by color [from yellow (gray) for large to blue (black) for small amplitudes].

around a semidisk body [26]. However, for $\theta=\pi/2$ the ratchet flow is composed from two alternative flows moving in opposite directions at the cell boundaries and the semidisk center (Fig. 5, bottom left-hand panel), such a flow is different from hydrodynamic flows with fixed velocity far from the body. For a qualitative description of the turbulent flow we may argue that the turbulence leads to a difference of pressures on different sides of the scatterer producing different resistances for different flow directions. This generates the ratchet flow for the ac force driving. In general the kinetic description is applicable when the interaction scattering length is large compared to the scatterer size, e.g., $v_T\tau_K > r_d$ for semidisks. At small values of τ_K this condition is broken (Figs. 3 and 5) and we have transition to the hydrodynamiclike regime where the theory (20) gives only approximate description. For the flashing cuts model the kinetic description remains always valid since the size of the scatterer is zero.

The dependence of the ratchet velocity on the interaction scattering time τ_K is shown in Fig. 6. The increase of inter-

actions (small τ_K) can change the sign of the flow in the x direction that is in a qualitative agreement with the theory (20). For weak interactions, the flows are opposite in x for polarization $\theta=0$ and $\theta=\pi/2$ while at strong interactions, they are collinear. Thus, in 2DEG in AlGaAs/GaAs hetero-junctions where interactions are relatively weak ($r_s \sim 1$) the flows are opposite for two polarizations in agreement with the experiment [19], but for other materials with stronger interactions (e.g., SiGe with $r_s \approx 6$) the flows may become collinear. We also note that at strong interactions the rescaled ratchet characteristics are not sensible to the temperature variation that indicates that we have an effective liquid flow with temperature independent viscosity.

V. DISCUSSION

In conclusion, our extensive numerical simulations show that even in the regime of strong interactions between particles a stationary ratchet flow is generated by monochro-
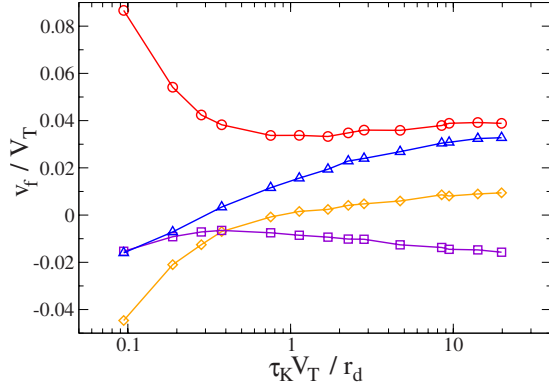
FIG. 6. (Color online) Dependence of the ratchet velocity v_f on the Kapral interaction scattering time τ_K in the semidisk model, numerical data are shown by symbols: $v_{f,y}/v_T$ (red circles) and $v_{f,x}/v_T$ (yellow diamonds) for $\theta = \pi/4$; $v_{f,x}/v_T$ (violet squares) for $\theta = 0$; $v_{f,x}/v_T$ (blue triangles) for $\theta = \pi/2$; other parameters are as in Fig. 3, top panel, curves are drown to adapt an eye.

matic driving in the asymmetric periodic arrays. The obtained result are well described by the analytical theory based on the kinetic equation for strongly interacting particles. It is interesting to note that for asymmetric arrays the tensor of conductivity becomes temperature dependent due to interplay of interactions and relaxation of high momentum harmonics [see Eq. (15) and discussion there]. It would be interesting to investigate the effects of interactions on ratchet transport in experiments similar to those of [19].

APPENDIX

Here, on the example of the flashing cuts model we give a more simple and heuristic derivation of the ratchet flow compared to the exact kinetic equation approach (1). In the regime of very strong interactions we can assume that the ensemble of particles is in a local equilibrium state and hence the distribution function can be written as

$$f(\mathbf{v}, t) = f_0[\mathbf{v} - \mathbf{v_0}(t)], \tag{A1}$$

where $\mathbf{v_0}(t)$ is the instantaneous velocity of the center of mass. We set here the particle mass $m = 1$. It is assumed that the interactions give rapid relaxation to the local equilibrium distribution $f_0[\mathbf{v} - \mathbf{v_0}(t)]$. The matrix of conductivity can be determined from the momentum balance between acceleration created by a small applied static force $\mathbf{F}$ and momentum loss on the asymmetric cut scatterer,

$$\frac{d\mathbf{p}}{dt} = \mathbf{F} - \frac{1}{\tau_c}[\langle \mathbf{V_c}(\mathbf{v}) f_0(\mathbf{v} - \mathbf{v_0}) \rangle - \mathbf{v_0}] = 0, \tag{A2}$$

where $\mathbf{V_c}(\mathbf{v})$ is the vector of average velocity after a scattering with the incident velocity $\mathbf{v}$. It is expressed via the scat-

tering probability $W(\mathbf{v}', v)$ (see the main text above) as $\mathbf{V_c}(\mathbf{v}) = \int d\mathbf{v}' W(\mathbf{v}', v)\mathbf{v}'$. This gives the relation

$$\langle \mathbf{V_c}(\mathbf{v}) f_0(\mathbf{v} - \mathbf{v_0}) \rangle = \int d\mathbf{v} \begin{pmatrix} \dfrac{2|\mathbf{v}|\theta(-v_x)}{\pi} - v_x\theta(v_x) \\ v_y\theta(v_x) \end{pmatrix} f_0(\mathbf{v} - \mathbf{v_0}), \tag{A3}$$

where $\theta(v)$ is the Heaviside function. In the linear response regime we can expand $\mathbf{v_0}$ to obtain $f_0(\mathbf{v} - \mathbf{v_0}) = f_0(\mathbf{v}) + f_0(\mathbf{v})\frac{\mathbf{v}\mathbf{v_0}}{T} + \cdots$. After integrating over the Maxwell distribution $f_0(\mathbf{v})$ we obtain

$$\langle \mathbf{V_c}(\mathbf{v}) f_0(\mathbf{v} - \mathbf{v_0}) \rangle = \int d\mathbf{v} \begin{pmatrix} \dfrac{2|\mathbf{v}|\theta(-v_x)}{\pi} - v_x\theta(v_x) \\ v_y\theta(v_x) \end{pmatrix} f_0(\mathbf{v}) \frac{\mathbf{v}\mathbf{v_0}}{T}$$
$$= \begin{pmatrix} -\dfrac{8 + \pi^2}{2\pi^2} v_{0,x} \\ \dfrac{1}{2} v_{0,y} \end{pmatrix}, \tag{A4}$$

where $\mathbf{v_0}$ is the velocity of the stationary flow. Then, the moment balance gives

$$\begin{pmatrix} v_{0,x} \\ v_{0,y} \end{pmatrix} = \tau_c \begin{pmatrix} \dfrac{2\pi^2}{8 + 3\pi^2} F_x \\ 2F_y \end{pmatrix}, \tag{A5}$$

and therefore $\sigma_{yy}/\sigma_{xx} = \tau_y/\tau_x = a_x/a_y = 3 + 8/\pi^2$ is in agreement with the kinetic theory result given in the main text. It is interesting to note that for the noninteracting particles we have $\sigma_{yy}/\sigma_{xx} = 3$ (see [18]).

To compute the ratchet flow we should expand the local velocity in Eq. (A1) up to the second order in the driving force $\mathbf{F}$: $\mathbf{v_0}(t) = \hat{\tau}_i\mathbf{F}(t) + \mathbf{v_f}$, $v_f = O(F^2)$ where τ_i are the above values τ_x, τ_y given by the linear response; we note that second frequency harmonics $e^{\pm i2\omega t}$ are eliminated by the time averaging. Then the time-averaged distribution function is

$$f(\mathbf{v}) = \langle f(\mathbf{v}, t) \rangle_t = f_0(\mathbf{v}) + f_0(\mathbf{v})\frac{\mathbf{v}\mathbf{v_F}}{T} + \frac{(\mathbf{v}\hat{\tau}_i\mathbf{F})^2 - T(\hat{\tau}_i\mathbf{F})^2}{4T^2} f_0(\mathbf{v}), \tag{A6}$$

where $f_0(\mathbf{v}) = \frac{1}{Z}\exp(-\frac{\mathbf{v}^2}{2T})$ is the Maxwell distribution and $\mathbf{v_F}$ is the average ratchet flow velocity. Again, the time-averaged momentum balance equation reads as

$$[\langle \mathbf{V_c}(\mathbf{v}) f(\mathbf{v}) \rangle - \mathbf{v_f}] = 0. \tag{A7}$$

Using Eq. (A7) we obtain from the second term the contribution $\langle \mathbf{V_c}(\mathbf{v}) f_0(\mathbf{v}) \frac{\mathbf{v}\mathbf{v_F}}{T} \rangle = [(1-a_x)v_{fx}, (1-a_y)v_{fy}]$ which is similar to the linear response term. The integration of the third Gaussian term gives the additional contribution $(F^2/8\sqrt{2\pi T})[(-\tau_x^2 \cos^2 \theta + \tau_y^2 \sin^2 \theta), 2\tau_x\tau_y \sin(2\theta)]$. Finally we obtain

$$\begin{pmatrix} v_{fx} \\ v_{fy} \end{pmatrix} = \frac{F^2}{8\tau_c\sqrt{2\pi T}} \begin{pmatrix} -\tau_x^3 \cos^2 \theta + \tau_x\tau_y^2 \sin^2 \theta \\ 2\tau_x\tau_y^2 \sin(2\theta) \end{pmatrix}. \quad \text{(A8)}$$

For $\omega \to 0$ these expressions are in agreement with Eqs. (20) obtained by the kinetic equation theory.

[1] F. Jülicher, A. Ajdari, and J. Prost, Rev. Mod. Phys. **69**, 1269 (1997).

[2] P. Reimann, Phys. Rep. **361**, 57 (2002).

[3] P. Hänggi and F. Marchesoni, e-print arXiv:0807.1283.

[4] E. M. Baskin, L. I. Magarill, and M. V. Entin, Sov. Phys. Solid State **20**, 1403 (1978) [Fiz. Tverd. Tela (Leningrad) **20**, 2432 (1978)].

[5] V. I. Belinicher and B. I. Sturman, Sov. Phys. Usp. **23**, 199 (1980) [Usp. Fiz. Nauk **130**, 415 (1980)].

[6] V. L. Alperovich, V. I. Belinicher, V. N. Novikov, and A. S. Terekhov, JETP Lett. **31**, 546 (1980).

[7] J. B. Majer, J. Peguiron, M. Grifoni, M. Tusveld, and J. E. Mooij, Phys. Rev. Lett. **90**, 056802 (2003); A. V. Ustinov, C. Coqui, A. Kemp, Y. Zolotaryuk, and M. Salerno, *ibid.* **93**, 087001 (2004).

[8] S. Matthias and F. Müller, Nature (London) **424**, 53 (2003).

[9] V. Studer, A. Pepin, Y. Chen, and A. Ajdari, Analyst (Cambridge, U.K.) **129**, 944 (2004).

[10] A. Lorke, S. Wimmer, B. Jager, J. P. Kotthaus, W. Wegscheider, and M. Bichler, Physica B **249-251**, 312 (1998).

[11] H. Linke, T. E. Humphrey, A. Löfgren, A. O. Sushkov, R. Newbury, R. P. Taylor, and P. Omling, Science **286**, 2314 (1999).

[12] A. M. Song, P. Omling, L. Samuelson, W. Seifert, I. Shorubalko, and H. Zirath, Appl. Phys. Lett. **79**, 1357 (2001).

[13] P. Olbrich, E. L. Ivchenko, T. Feil, R. Ravash, S. D. Danilov, J. Allerdings, D. Weiss, and S. D. Ganichev, e-print arXiv:0808.1983.

[14] A. D. Chepelianskii and D. L. Shepelyansky, Phys. Rev. B **71**, 052508 (2005).

[15] G. Cristadoro and D. L. Shepelyansky, Phys. Rev. E **71**, 036111 (2005).

[16] M. V. Entin and L. I. Magarill, Phys. Rev. B **73**, 205206 (2006).

[17] A. D. Chepelianskii, Eur. Phys. J. B **52**, 389 (2006).

[18] A. D. Chepelianskii, M. V. Entin, L. I. Magarill, and D. L. Shepelyansky, Eur. Phys. J. B **56**, 323 (2007).

[19] S. Sassine, Y. Krupko, J.-C. Portal, Z. D. Kvon, R. Murali, K. P. Martin, G. Hill, and A. D. Wieck, Phys. Rev. B **78**, 045431 (2008).

[20] E. Abrahams, S. V. Kravchenko, and M. P. Sarachik, Rev. Mod. Phys. **73**, 251 (2001).

[21] D. van der Meer, P. Reimann, K. van der Weele, and D. Lohse, Phys. Rev. Lett. **92**, 184301 (2004).

[22] D. E. Feldman, S. Scheidl, and V. M. Vinokur, Phys. Rev. Lett. **94**, 186809 (2005); B. Braunecker, D. E. Feldman, and J. B. Marston, Phys. Rev. B **72**, 125311 (2005).

[23] A. Malevanets and R. Kapral, in *Novel Methods in Soft Matter Simulations*, edited by M. Karttunen, I. Vattulainen, and A. Lukkarinen, Lecture Notes in Physics Vol. 640 (Springer, Berlin, 2004), p. 116.

[24] W. G. Hoover, *Time Reversibility, Computer Simulation, and Chaos* (World Scientific, Singapore, 1999).

[25] A. D. Chepelianskii, A. S. Pikovsky, and D. L. Shepelyansky, Eur. Phys. J. B **60**, 225 (2007).

[26] L. D. Landau and E. M. Lifshitz, *Hydrodynamics* (Nauka, Moskow, 1986).